Magnetic Resonance Imaging Evidence for Widespread Orbital Dysinnervation in Dominant Duane's Retraction Syndrome Linked to the DURS2 Locus

Joseph L. Demer,[1,2,3,4] *Robert A. Clark,*[1] *Key-Hwan Lim,*[1,5] *and Elizabeth C. Engle*[6,7,8,9]

Purpose. High-resolution, multipositional magnetic resonance imaging (MRI) was used to demonstrate extraocular muscles (EOMs) and associated motor nerves in Duane retraction syndrome (DRS) linked to the DURS2 locus on chromosome 2.

Methods. Five male and three female affected members of two autosomal dominant DURS2 pedigrees were enrolled in the study. Coronal T_1-weighted MRI of the orbits was obtained in multiple gaze positions, as well as with heavy T_2 weighting in the plane of the cranial nerves. MRI findings were correlated with motility.

Results. All subjects had unilateral or bilateral limitation of abduction, or of both abduction and adduction, with palpebral fissure narrowing and globe retraction in adduction. Orbital motor nerves were typically small, with the abducens nerve (cranial nerve [CN]6) often nondetectable. Lateral rectus (LR) muscles were structurally abnormal in seven subjects, with structural and motility evidence of oculomotor nerve (CN3) innervation from vertical rectus EOMs leading to A or V patterns of strabismus in three cases. Four cases had superior oblique, two cases superior rectus, and one case levator EOM hypoplasia. Only the medial and inferior rectus and inferior oblique EOMs were spared. Two cases had small CN3s.

Conclusions. DRS linked to the DURS2 locus is associated with bilateral abnormalities of many orbital motor nerves, and structural abnormalities of all EOMs except those innervated by the inferior division of CN3. The LR may be coinnervated by CN3 branches normally destined for any other rectus EOMs. Therefore, DURS2-linked DRS is a diffuse congenital cranial dysinnervation disorder involving but not limited to CN6. (*Invest Ophthalmol Vis Sci.* 2007;48:194–202) DOI:10.1167/iovs.06-0632

Duane retraction syndrome (DRS) is characterized by congenital abduction deficit, narrowing of the palpebral fissure on adduction, and globe retraction with occasional upshoot or downshoot in adduction.[1] Early electrophysiologic studies suggested absence of normal abducens (cranial nerve [CN]6) innervation to the lateral rectus (LR) muscle as the cause of DRS, with paradoxical LR innervation in adduction.[2,3] Absence of CN6 and motor neurons has been confirmed in one sporadic unilateral[4] and another bilateral autopsy case of DRS.[5] Parsa et al.[6] first used magnetic resonance imaging (MRI) to demonstrate absence of the subarachnoid portion of CN6 in DRS, a finding that has been confirmed in 6 of 11 additional cases,[7] and later correlated with the presence of residual abduction in multiple cases.[8,9]

Innervation of the LR by CN6 is deficient in both DRS and CN6 palsy, although unlike CN6 palsy, the eyes in central gaze are frequently aligned in DRS.[10] This evidence for contractile tonus in the LR suggests that the involved LR is either solely, or coinnervated, by a branch of the oculomotor nerve (CN3) as supported by the autopsy studies.[4,5] No direct anatomic evidence of LR innervation by CN3 in DRS has been available in living subjects. It is now possible to investigate such innervation in living subjects by high-resolution MRI, which affords the opportunity for detailed study of the functional anatomy of EOMs and nerves.[11,12]

Although most cases of DRS are sporadic, approximately 10% are estimated to be familial.[10,13] Only one genetic locus for isolated DRS has been established by linkage analysis—the DURS2 locus on 2q31. Two pedigrees have been reported in which the DRS phenotype segregated with the DURS2 locus as an autosomal dominant trait.[13,14] The present study was performed to characterize the endophenotype, the internal phenotype of the structure and function of EOMs, as well as orbital innervation, in two additional families with autosomal dominant DRS that are demonstrated in the companion paper to map to the DURS2 locus.[15]

Methods

Subjects and Clinical Examination

Two unrelated pedigrees, FY and JH, were identified that cosegregated the DRS phenotype with the DURS2 locus. The structure and mapping data for pedigrees FY and JH are presented in the companion paper.[15] The living members of these pedigrees who had inherited all or a portion of the disease-associated DURS2 allele were invited to participate in an on-going clinical and MRI study of inherited congenital cranial dysinnervation disorders.[15] Because of the need for prolonged visual fixation, however, only participants older than 10 years qualified for enrollment in the MRI portion of the study. Paid normal control subjects were recruited by advertising. To assess possible nonspecific effects of the strabismus surgeries that many subjects with *DURS2* had undergone before entering this study, an additional control group comprised six strabismic adults without DRS who underwent MRI before and after conventional strabismus surgery. Clinical examinations were performed and MR images collected from volunteers who agreed to participate and gave written informed consent to a protocol conforming to the Declaration of Helsinki and approved by relevant institutional review boards. Control and affected subjects underwent examination of corrected visual acuity, ocular motility, eyelid structure

From the Departments of [1]Ophthalmology and [2]Neurology, Jules Stein Eye Institute, and the [3]Bioengineering and [4]Neuroscience Interdepartmental Programs, University of California, Los Angeles, California; the [5]Department of Ophthalmology, College of Medicine, Ewha Womans University, Seoul, Korea; [6]Programs in Genomics and [7]Department of Neurology, Children's Hospital, Boston, Massachusetts; and [8]Department of Neurology and [9]Program in Neuroscience, Harvard Medical School, Boston, Massachusetts.

Supported by U.S. Public Health Service, National Eye Institute: Grants EY13583, EY08313, and EY00331. JLD is the recipient of an unrestricted award from Research to Prevent Blindness and is the Leonard Apt Professor of Ophthalmology.

Submitted for publication June 9, 2006; revised August 23, 2006; accepted November 15, 2006.

Disclosure: **J.L. Demer**, None; **R.A. Clark**, None; **K.-H. Lim**, None; **E.C. Engle**, None

The publication costs of this article were defrayed in part by page charge payment. This article must therefore be marked "*advertisement*" in accordance with 18 U.S.C. §1734 solely to indicate this fact.

Corresponding author: Joseph L. Demer, Jules Stein Eye Institute, 100 Stein Plaza, UCLA, Los Angeles, CA 90095-7002; jld@ucla.edu.

and function, binocular alignment, anterior segment anatomy, and ophthalmoscopy. Ophthalmic histories were obtained, with corroboration of previous ocular surgeries from operative records, when possible.

Magnetic Resonance Imaging

MRI was performed with a 1.5-T scanner (Signa; General Electric, Milwaukee, WI). Orbital imaging was performed as described elsewhere in detail,[16–20] using surface coils (Medical Advances, Milwaukee, WI) and fixation targets. Imaging posterior to the orbital apex in some subjects was performed with the standard head coil. When surface coils were used, images of 2 mm thickness in a matrix of 256 × 256 were obtained over a field of view of 6 to 8 cm for a resolution in plane of 234 to 312 μm. Imaging of subarachnoid cranial nerves was performed in 1-mm thickness image planes using the heavily T_2-weighted FIESTA sequence, which provides good contrast against the surrounding cerebrospinal fluid.[11,21] In-plane resolution was 195 μm over a 10-cm field of view (matrix, 512 × 512) with 10 excitations. Magnetic resonance angiography was performed using the head coil in one subject with DURS2, and reconstructed in conventional fashion.

Digital MR images were quantified by using the programs NIH Image 1.59 and ImageJ 1.33μ (available by ftp at zippy.nimh.nih.gov/ or at http://rsb.info.nih.gov/nih-image; developed by Wayne Rasband, National Institutes of Health, Bethesda, MD). In coronal planes, the location of each rectus EOM was described by the "area centroid" using a published method.[22] Cross section determinations were made in ImageJ, which, because of a difference in perimeter treatment, produces different area values than does NIH Image 1.59, which in turn produces different area values than some other versions of NIH Image. Centroid determinations do not differ between NIH Image and ImageJ. The globe center was determined as previously described.[18] Rectus EOM positions were then translated to place the three dimensional (3-D) coordinate origin at globe center. Coronal plane rectus pulley locations were determined from the EOM centroids at published anteroposterior positions.[18] Inferior oblique (IO) muscles were analyzed using outlined cross sections in quasisagittal images, as described elsewhere in detail.[23] Optic nerve (ON) cross sections were analyzed in the first image plane immediately posterior to the globe.[24]

We computed rectus EOM volumes by summing the cross sections for each EOM in the image plane containing the junction of the globe and ON and the next five contiguous image planes posterior to this plane and then multiplying by the image plane thickness of 2 mm. Although this approach fails to account for EOM volume deep to the image planes collected, these data were available for every subject, and the technique was identical with that used for published data in control subjects and subjects with CFEOM1.[11] This technique avoids the confounding problem of defining the borders of highly dysplastic deep portions of EOMs, such as the LR, in several subjects with DRS.

Results

Subjects

Eleven members of pedigrees FY and JH consented to participate. Of these, eight participants had DRS and harbored the DRS-associated allele (subjects 1–4 and 8–11). These eight subjects include five males and three females with an average age of 39 ± 6 (mean ± SE; range 2–76) years. The remaining three participating family members were clinically unaffected. Subject 5 was a 6-year-old boy who harbored the DRS-associated allele and was an obligate carrier of the DURS2 mutation. Subject 7 was a 50-year-old woman who harbored a portion of the DRS-associated allele, and it is unknown whether she carried the DURS2 mutation. Subject 6 was a 23-year-old woman who did not carry the DRS-associated allele but was enrolled in the clinical portion of the study because she traveled to UCLA with her family. All 11 participating family members underwent clinical examinations. General characteristics of these subjects are summarized in Table 1.

Six strabismic subjects without DRS of average age 46 ± 8 (SEM) years underwent MRI of the orbits before and after surgery for horizontal strabismus. This control group was included to determine whether strabismus surgery alters EOM volumes significantly. In this group, mean (±SEM) corrected visual acuity was 0.01 ± 0.04 logMAR in the right eye, and −0.01 ± 0.02 logMAR in the left eye. All subjects in this group underwent surgery on at least two horizontal rectus muscles, and one subject also underwent bilateral IO recession.

Detailed orbital MRI was performed in subjects 1 to 4, and 9 to 11, and MRI of cranial nerves in the skull base was performed in subjects 4, 9, 10, and 11. Subject 7 consented to and attempted orbital MRI, but the study was limited due to

Table 1. Characteristics of Study Participants

Subject	Pedigree	Age (y)	Sex	Corrected Visual Acuity		Horizontal Alignment	DRS Type		MRI	
				Right (logMAR)	Left (logMAR)		Right	Left	Orbital	Brain Stem
1	FY, V:6	39	M	0.0	0.0	A-ET, LHT, limited up OD	3	None	Yes	No
2	FY, V:14	43	M	0.2	0.0	A-XT, RHT	3	3	Yes	No
3	FY, V:12	45	M	0.0	0.0	XT, limited down OS	3	3	Yes	No
4	FY, V:3	52	F	0.0	0.2	λXT, RHT, limited down OU	3	3	Yes	Yes
5	FY, VI:4	6	M	0.6	0.6	Unaffected carrier	None	None	No†	No
6	FY, VI:6	23	F	ND	ND	Unaffected	None	None	No	No
7	FY, V:5	50	F	−0.1	0.0	Unaffected	None	None	No‡	No
8	JH, V:1	1	M	ND	ND	XT	1	3	No†	No
9	JH, IV:3	24	F	0.05	0	V-XT	3	3	Yes	Yes
10	JH, III:3	52	M	0	0	λET	3	1	Yes	Yes
11	JH, III:6	56	F	0.1	0.1	ET	3	1	Yes	Yes
Mean		39		0.04*	0.04*					
SEM		6		0.02*	0.03*					

Quantitative acuity could not be obtained in preverbal Subject 8. ET, esotropia; A-ET, A pattern esotropia; A-XT, A pattern exotropia; LHT, left hypertropic; RHT, right hypertropia; V-XT, exotropia; XT, exotropia.

* Acuities include only subjects manifesting the DRS phenotype.

† Subject too young for participation in MRI portion of the study.

‡ MRI aborted secondary to claustrophobia.

claustrophobia, and images were inadequate to trace intraorbital innervation. Subjects 5 and 8 were too young to participate in the MRI portion of the study, which has a minimum age for participation of 10 years. Subject 6 did not undergo MRI, because she did not have DRS and did not harbor the disease-associated haplotype.

Thirteen normal volunteers underwent MRI of the cranial nerves in the skull base. Normal control subjects were of average age 22 ± 4 (mean ± SD, range 17–26) years. All control subjects had normal ocular and lid motility and visual acuity in each eye correctable to 0 logarithm of the minimum angle resolvable in arc minutes (logMAR, 20/20) or better.

Clinical Findings in DURS2

Mean corrected letter visual acuity in the group was identical in the left and right eyes of affected subjects (Table 1), and averaged 0.04 logMAR (20/20$^-$ Snellen). The maximum interocular acuity difference observed was 0.2 logMAR, found in subjects 2 and 4, indicating minimal to no amblyopia in affected subjects. Quantitative acuity could not be obtained in subject 8, age 1 year, who could not identify optotypes.

With the exception of subject 1, who exhibited unilateral motility abnormalities in the right eye only, affected subjects exhibited bilateral, albeit often asymmetrical, manifestations of DRS. Posterior displacement of the globe, termed retraction, was evident on attempted adduction of all affected eyes except for the right eye of subject 4. Although globe retraction was associated with narrowing of the palpebral fissure on attempted adduction, blepharoptosis in central gaze was present only in subject 4, in whom it was bilateral and had required surgical correction before the study. Five of the affected subjects had undergone two or three surgeries each for strabismus correction before the study. Affected subjects 2, 8, and 10 had not undergone prior ocular surgery.

The common clinical classification by Huber of DRS consists of three groups: type 1, with limitation of abduction only; type 2, with limitation of adduction only; and type 3, with limitation of both ab- and adduction.[2,25] As noted in Table 1, 1 right and 2 left eyes were classified as DRS type 1, and 10 eyes exhibited DRS type 3. Four affected participants had bilateral type 3, three had unilateral type 3 and unilateral type 1, and one was unilaterally affected with type 3. No eye exhibited the limitation of adduction only characteristic of type 2.

As indicated in Table 1, three affected subjects exhibited esotropia in central gaze, and the other five exhibited exotropia. The strabismus was unaltered (concomitant) during vertical gaze changes in subjects 5 and 8 only, but varied with vertical gaze in the other subjects. Subjects 1, 2, 4, and 10 had incomitant horizontal strabismus evocative of the letter A or Greek letter λ because the eyes were in a more divergent position in down gaze than in up gaze. In subjects 1 and 10, esotropia was reduced in down gaze, whereas in subjects 2 and 4, exotropia was increased in down gaze. In several of these subjects, this A or λ pattern was highly suggestive of aberrant innervation of the lateral rectus (LR) muscle during infraduction, and LR inhibition during attempted supraduction (Fig. 1). Subject 3 exhibited limited infraduction of the left eye and so could not be evaluated for vertical incomitance of his horizontal strabismus.

Orbital Imaging Findings in DURS2-Linked DRS

Rectus EOMs. Despite prior strabismus surgery in several cases, orbital MRI was thought to provide a reasonable reflection of the sizes and positions of the EOM bellies because surgery is largely confined to the region of the insertional tendons. This impression was confirmed in the strabismic control group without DURS2 by demonstration that EOM volumes did not change significantly after conventional surgery for horizontal strabismus (Table 2). Mean volumes of each of the four rectus EOMs in the six contiguous image planes including and posterior to the junction of the globe and ON did not significantly differ between control subjects, and subjects with DURS2 ($P > 0.05$). The volume measurement did not, however, incorporate rectus EOMs in their most apical portions.

Structural abnormalities of the LR were common among subjects with DURS2. All had structural abnormalities of the left LR, including posterior hypoplasia in subject 1, vertical splitting in subjects 2 to 4 and 9 and 11, and internal bright signal in subject 10. Structural abnormalities of the right LR were common but not universal. Right LR abnormalities included posterior hypoplasia in subject 1, posterior disorganization in subjects 3 and 4, and internal bright signal in subject 10. The anterior portion of the LR was typically normal, but the deep portion was split into superior and inferior portions (Figs. 2, 3), one or both of which were hypoplastic (Fig. 3). It should be noted that LR volume measurements in Table 2 do not include the deep portion, where structural abnormalities were most severe in pedigree FY. Quasi-sagittal MRI distinguished a lengthy separation between the superior and inferior parts of the LR along its length (Fig. 4).

Although structural EOM abnormalities were confined to the LR in pedigree JH, other EOMs were commonly abnormal in pedigree FY. Subjects in pedigree FY exhibited hypoplasia of at least one superior oblique (SO) muscle; this was bilateral in subjects 1 to 3 and in the left eye only of subject 4 (Fig. 2). The left SO of subject 4 also exhibited dysplasia with vertical elongation in the region of an abnormal slip of the dysplastic levator palpebrae superioris (LPS) muscle (Fig. 2). Subjects 1 and 4 of pedigree FY also had unilateral hypoplasia of the superior rectus (SR) muscle (Fig. 2). The normal configuration of the SO and LPS EOMs may be seen for comparison in Figure 3, illustrating the right orbit of subject 4.

FIGURE 1. A-pattern in subject 4, showing esotropia in attempted upward gaze, and exotropia in central and downward gaze. Note limitation of vertical gaze, and left hypotropia. The upper eyelid configuration was created at surgery for blepharoptosis. There was prior strabismus surgery.

TABLE 2. Muscle Volumes in Subjects with DURS2-Linked DRS

	Control Subjects $n = 9$ Volume (mm^3)		Strabismic Controls, before Surgery $n = 6$ Volume (mm^3)		Strabismic Controls, after Surgery $n = 6$ Volume (mm^3)		Subjects with DURS2, $n = 7$ Volume (mm^3)	
Muscle	**Mean**	**SEM**	**Mean**	**SEM**	**Mean**	**SEM**	**Mean**	**SEM**
Medial rectus	395	16	362	17	369	14	376	12
Superior rectus	370	32	320	12	336	14	374	16
Lateral rectus	428	15	376	22	374	17	385	17
Inferior rectus	385	12	334	16	327	15	387	15

Subjects contributed data from both orbits where available. Volumes for rectus EOMs include contributions from six contiguous image planes extending posteriorly beginning at the globe-optic nerve junction. None of the differences reached statistical significance ($P > 0.05$).

Oblique EOM Size. The size of the IO was not systematically determined because quasisagittal imaging was performed only in three EOMs of two subjects (subjects 2 and 4), in whom mean (± SEM) IO volume was significantly subnormal at 161 ± 2.2 microliters ($P < 0.0001$). Control IO volume averaged 301 ± 11 mL ($n = 55$).

For comparability to the published literature, SO size was assessed by maximum cross section in quasicoronal image planes. Averaging over both eyes of 10 normal subjects, mean maximum SO cross section was 18.8 ± 0.7 mm^2 (SEM). In DURS2, the mean maximum SO cross section was significantly smaller than normal at 14.2 ± 1.9 mm^2 ($P < 0.025$).

Rectus Muscle Paths. Paths of the rectus EOMs were determined from area centroids in multiple contiguous image planes. The EOMs pass through their connective tissue pulleys, so that the anterior locations of these paths indicate the respective pulley locations in the coronal plane.[20] Because subjects with DURS2 were typically unable to achieve eccentric gaze positions, no inflections in rectus EOM paths were present to identify the anteroposterior coordinates of the rectus pulleys as is possible in normal subjects. It therefore was assumed that the anteroposterior coordinates of the rectus pulleys are the same as those known for normal subjects.[20] This was considered reasonable, since variations in anteroposterior coordinates would on geometric grounds be expected to have only a small effect on horizontal and vertical pulley coordinates in central gaze. After 3-D averaging of the paths of the IR, MR, and LR in subjects with DURS2, the horizontal coordinates were determined at the anteroposterior locations of normal rectus pulleys. This analysis indicated that the 3-D coordinates of all rectus pulleys in DURS2 do not differ significantly from normal.

Imaging of Intraorbital Motor Nerves. Since the posterior orbit is less susceptible to motion artifacts from eye movement than is the anterior orbit, it was possible to examine in the deep orbit the motor nerves to the EOMs in image planes of 1.5- to 2-mm thickness, and field of view 6 to 8 cm. The superior division of CN3 was difficult to follow and was not analyzed systematically. The inferior division of CN3 and its individual branches are normally prominent in the orbit.[11,12] Most posteriorly, it may be seen on MRI to divide into an inferior trunk, one branch of which bifurcates repeatedly as it travels anteriorly on the global surface of the IR that enters the EOM. The inferior trunk has a lateral branch that courses anteriorly along the lateral border of the IR and enters the IO at the point where it crosses the IR. The medial trunk of the inferior division on CN3 normally crosses inferior to the ON to make a prominent entry into the global surface of the MR. The

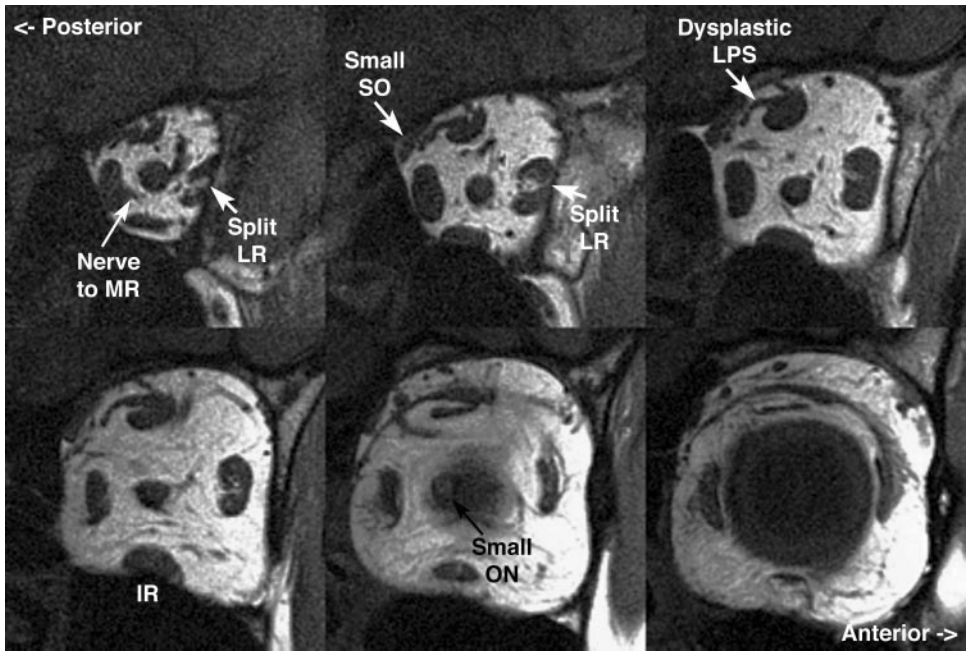

FIGURE 2. Quasicoronal MRI planes 2 mm thick of left orbit of subject 4 from pedigree SB, demonstrating a small, dysplastic SO, and dysplasia of the LPS, forming an abnormal slip extending toward the SO. The LR muscle was split into superior and inferior portions. The ON was small.

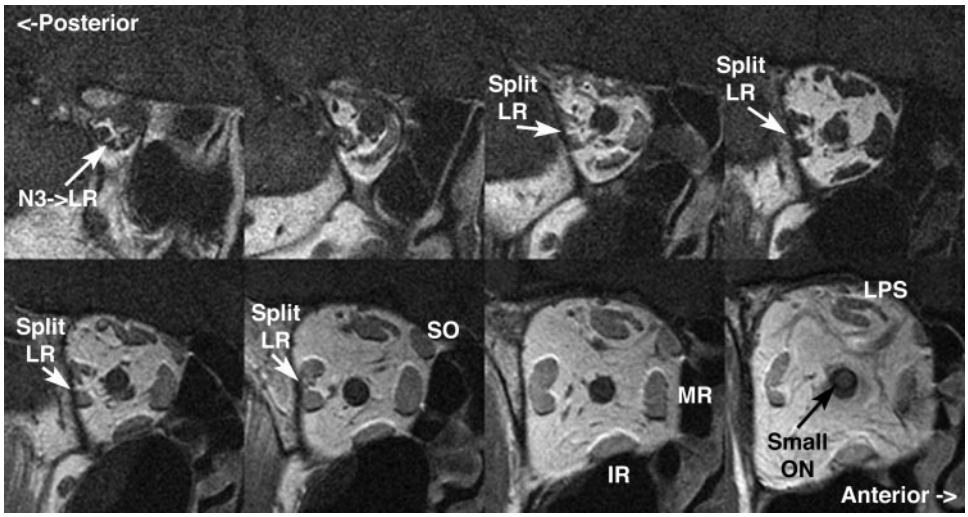

FIGURE 3. Quasicoronal MRI planes 2 mm thick of the right orbit of subject 4 from pedigree FY, demonstrating marked dysplasia of the LR, with continuity and apparent innervation of the LR by a branch of the inferior division of the oculomotor nerve (N3). The deep LR was also hypoplastic. The SO was of normal size. The LPS was mildly dysplastic. Note the small ON cross section in the most anterior image at lower right.

normal CN6 is smaller than the branches of CN3, but typically may be seen on MRI to bifurcate repeatedly to form a manifold on the global surface of the LR as it courses anteriorly to innervate the LR. Since normal intraorbital motor nerves to individual EOMs are represented by one or at most a few pixels in the coronal image planes used in this study, the images were regarded as insufficiently precise for quantitative analysis of motor nerve size. However, qualitative impressions were consistently obtained and are illustrated herein Assessments were confirmed by evaluation of multiple contiguous MRI planes to trace the paths of presumed nerves to their target EOMs.

The CN6 was absent or below detection in the right orbits of subjects 1, 4, and 11, and appeared smaller than normal in subjects 9 and 10. All the foregoing exhibited DRS type 3 on the right. The CN6 was absent or below detection in the left orbit of subjects 10 and 11, both of whom had DRS type 1 in the affected orbit. In subject 1, who exhibited no clinical evidence of DRS on the left, the left CN6 was identified to be present in the orbit despite LR hypoplasia. All remaining subjects imaged had type 3 DRS on the left, and had identifiable CN6 in the orbit. When present, CN6 innervated the superior belly of the split LR. In the right orbit of subjects 3, 4, 6, 7, and 8 and in the left orbit of subjects 1, 4, 9, and 10, a branch of CN3 was in close contact with the inferior belly of the LR. As illustrated in Figure 3, the intimate contact of the inferior division of CN3 with the LR suggested that the CN3 branch entered the EOM, although the limited resolution of MRI precludes confirmation of actual innervation at the level of the EOM fibers. The MR and IR were innervated normally by branches of CN3 in all orbits imaged.

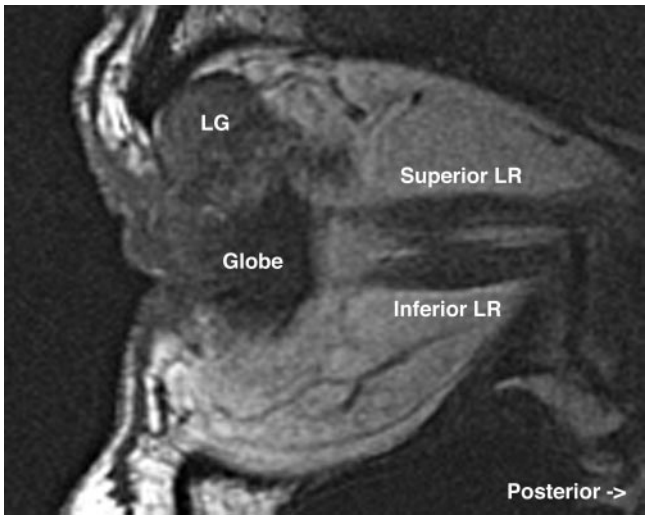

FIGURE 4. Quasisagittal, T_1-weighted MRI of subject 4 showing longitudinal splitting of the left LR into superior and inferior portions, with intercalated bright signal consistent with orbital fat: 312-μm resolution in 2-mm image plane. LG, orbital lobe of the lacrimal gland.

Imaging of Intracranial Motor Nerves. Heavily T_2-weighted imaging of the skull base region was conducted in 1-mm-thick slices at 390-μm resolution in the plane of the optic chiasm and major cranial nerves to the orbit. This technique has just sufficient resolution to demonstrate the normal CN6s coursing anteriorly from the pons (Fig. 5), whereas it easily and consistently demonstrates the larger course of the CN3s of normal subjects (Fig. 6).[11]

The heavily T_2-weighted imaging technique demonstrated the CN6 in all normal subjects (Fig. 5, left). In adjacent sections, CN6 could be traced from the pons across the cerebrospinal fluid space to the clivus in every normal subject. The CN6 was not demonstrable bilaterally using the identical technique in subjects 4, 10, and 11. In subject 9, the right CN6 was hypoplastic, whereas the left CN6 was not definable within a dysplastic region spanning the subarachnoid space. The remaining affected subjects did not undergo this imaging.

The heavily T_2-weighted imaging technique readily demonstrated the CN3 in multiple contiguous image planes in all 13 normal subjects (Fig. 6, left). Imaging capable of demonstrating CN3 at the brain stem was performed in subjects 4, 9, 10, and 11. The right CN3 was unilaterally hypoplastic in affected subjects 9 and 10, and appeared qualitatively normal in subjects 4 and 11. Averaging bilaterally, mean $\pm$ SEM. CN3 width was 1.55 ± 0.18 mm in affected subjects, significantly smaller than the width of 2.10 ± 0.07 mm in normal subjects ($P < 0.005$).

Optic Nerve. Despite the normal ophthalmoscopic appearance of the ON in all affected subjects, the coronal plane MRI was notable for the appearance of subnormal ON size in several subjects (Fig. 2). Because the ON cross section normally decreases from anterior to posterior in the orbit due to the reduction of connective tissues surrounding the axon bundles,[24] ON cross sections were analyzed at the 2-mm-thick image plane thickness closest to the globe-ON junction. Mean ($\pm$ SEM) cross section of the ON in 14 orbits with DURS2 was 6.85 ± 0.36 mm^2, significantly smaller than the mean cross section of 18 normal control orbits of 9.19 ± 0.46 mm^2 ($P < 0.001$).

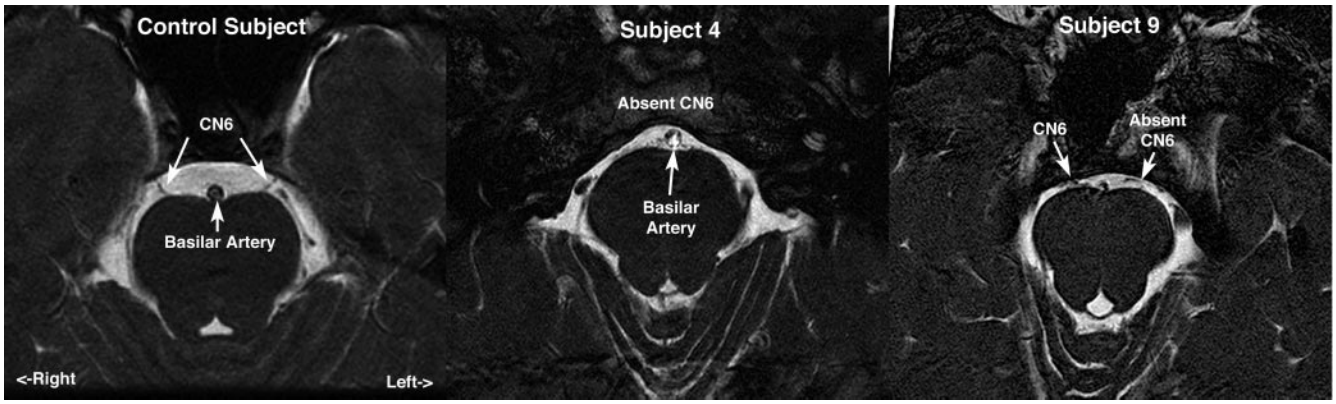

FIGURE 5. Oblique, axial, heavily T_2-weighted MR images showing at *left* the normal course of the abducens nerve (CN6 dark) from the pons highlighted against the bright signal of the surrounding cerebrospinal fluid. In contrast, the CN6s of subject 4 with DURS2 appeared absent and the left CN6 of subject 9 was shown to be absent by the identical technique. In each panel, CN6 was demonstrated in the optimal 1-mm-thick image plane in which it appeared or was expected to appear based on surrounding landmarks.

Functional Evidence for Misinnervation. Abnormal patterns of EOM contraction provided evidence of misinnervation in several illustrative cases. Subject 1 had the clinical phenotype of DRS type 3 on the right, with limited abduction, adduction, and supraduction, downshoot on adduction, and A-pattern esotropia (Table 1). Coronal plane imaging was performed during target fixation by the left eye to control innervational effort, and was repeated in attempted abduction, central gaze, and attempted adduction (Fig. 7). Although there was some abduction of the right eye, the right LR exhibited modest contractile thickening mainly in its more anterior portion, with little contractile change in the deep orbit (Fig. 7). Although right MR exhibited robust contractile thickening in adduction (Fig. 7), adduction was slightly limited. However, in adduction, the right eye exhibited a downshoot that was associated with an increase in IR cross section suggestive of active contraction (Fig. 7). This inference of anomalous IR contraction on adduction is supported by the absence of an increase in SO cross section, the other EOM that would normally mediate infraduction. Anterior views near the level of the rectus pulleys showed no evidence of horizontal rectus EOM sideslip, indicating that the downshoot was not due to a "bridle effect" during horizontal rectus co-contraction.

Ductions of the left eye of subject 1 appeared clinically normal. However, MRI of the left orbit at 234-μm resolution indicated the presence of CN6 but hypoplasia of the deep LR belly (Fig. 8). This observation suggests that the DRS endophenotype (internal phenotype) of LR hypoplasia was bilateral in subject 1. Apparently the presence of CN6 innervation to the hypoplastic left LR in subject 1 was sufficient to maintain an apparently normal clinical motility phenotype on the left. The absence of the right CN6 was associated with the right DRS type 3 in subject 1.

DISCUSSION

Confirmation and Extension of DURS2 Phenotype

Similar to the two previously reported DURS2 pedigrees, the eight subjects examined with DURS2 all exhibited either DRS type 3 bilaterally or unilaterally, or DRS type 3 in one eye and DRS type 1 in the other, accompanied by globe retraction on adduction of at least one eye. Of note, the right eye of subject 4 with limited abduction and adduction did not retract, highlighting the potential phenotypic overlap between DRS and horizontal gaze palsy. No subject or eye exhibited DRS type 2 (isolated limitation of adduction). The cosegregation of DRS types 1 and 3 but not 2 has also been noted in the two previously reported DURS2 pedigrees, as well as in patients with Duane radial ray syndrome resulting from mutations in *SALL4*.[26] Thus, although DRS types 1 and 3 can result from the same primary genetic defect, DRS type 2 appears to be a unique disorder.

In subject 1, MRI revealed an absent CN6 on the right, and abnormalities of the LR in both orbits, despite the absence of clinical manifestations of DRS in the left eye. This suggests that

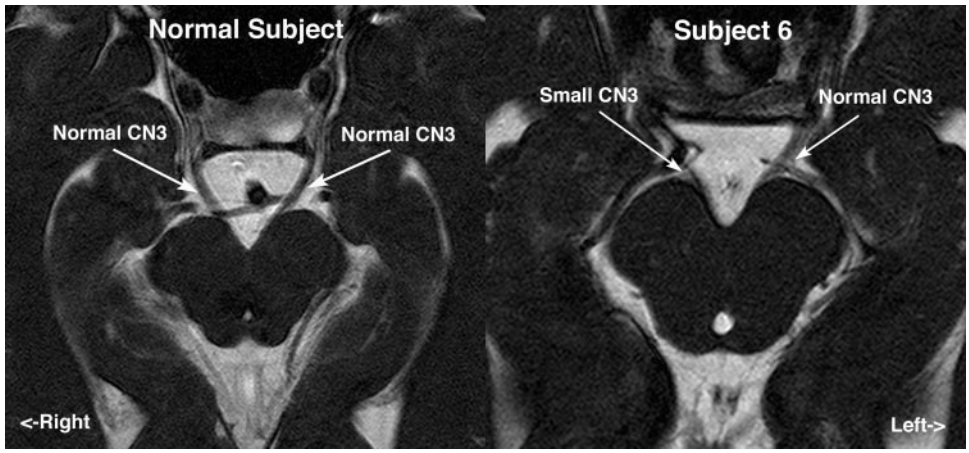

FIGURE 6. Heavily T_2-weighted axial MR images of 1-mm thickness at the level of the midbrain obtained in the plane of the optic chiasm. In all normal subjects, the oculomotor nerve (CN3) was prominent in multiple contiguous image planes. In subject 6 with DURS2, the right CN3 was hypoplastic.

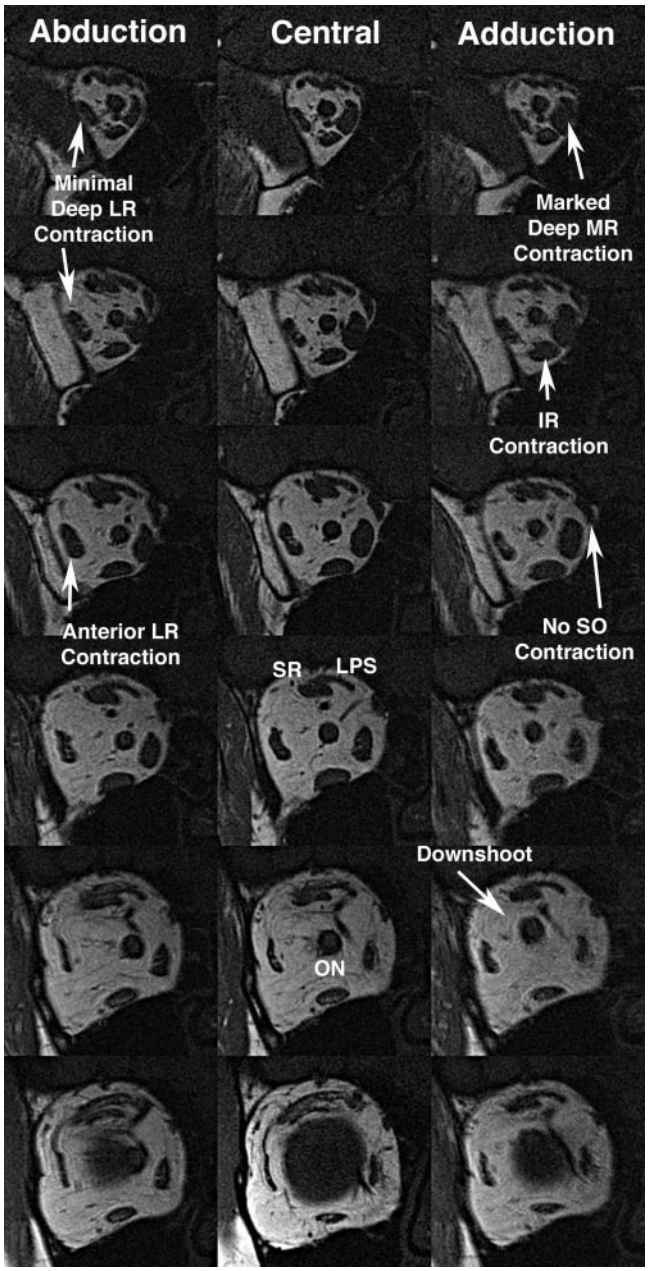

FIGURE 7. Coronal MRI of the right orbit of subject 1 with the clinical phenotype of unilateral DRS type 3 on the right. Image planes 2-mm thick spaced by 2 mm, resolution 312 μm in planes arranged from posterior at top to anterior at bottom. Fixation was by the clinically normal left eye. Note the minimal increase in the deep LR cross section on abduction, with a moderate increase in the anterior LR cross section on abduction. Although the deep MR exhibited a marked contractile increase in cross section, the eye adducted little, and the elevated position of the globe–ON junction indicated a downshoot. Note the increase in IR cross section in adduction suggestive of IR contraction, without corresponding increase in SO cross section. Note the normal positions of the MR and LR muscles near the globe–ON junction (*bottom row*), indicating normal stability of the horizontal rectus pulleys and ruling out sideslip as the cause of the downshoot in adduction.

mutations in the DURS2 gene can result in orbital abnormalities consistent with DRS that are clinically silent (an endophenotype). Such an endophenotype may also occur in subject 5, who carried the DRS-associated allele but was clinically unaffected. Unfortunately, he was too young for participation in the MRI portion of this study.

Although most subjects with DURS2 had undergone strabismus surgery, six of the eight nevertheless exhibited A- or V-pattern strabismus. This prior surgery created no apparent change in rectus EOM volumes, as determined by the current technique, since volumes in DURS2 did not differ significantly from those in normal control subjects or in strabismic subjects without DRS, either before or after strabismus surgery. Three of the eight subjects with DURS2 exhibited limitation of vertical gaze in one or both eyes, similar to two of the 25 cases of hereditary DRS from the original DURS2 pedigree[13] reported by Chung et al.[27] Unlike these original 25 cases, however, none of the eight patients in the current report exhibited dense amblyopia, and only subject 4 exhibited blepharoptosis. Of note, these additional symptoms were found in subsets of the 25 patients reported by Chung et al., and clustered within smaller family units, suggesting that they may represent the influence of modifying genes. Whereas one of the current 8 subjects had Klippel-Feil anomaly, seizures and deafness were each found in 1 of the 25 patients in Chung et al.; these may represent rare manifestations of the DURS2 gene or may be incidental findings.

The present MRI findings confirm limited autopsy[4,5] and electromyographic[2,3,28] reports of CN6 aplasia with peripheral misinnervation of the LR by CN3 and extend these findings to demonstrate a novel variety of patterns of mis- and coinnervation of the inferior portion of the LR belly by CN3 branches normally destined for the IR, MR, and SR muscles. Although the resolution of the current MRI technique was insufficient to demonstrate actual neuromuscular junctions and trace peripheral axons, it was possible to demonstrate contractile changes in the affected LR associated with innervational effort determined by target fixation by the fellow eye.

Paradoxical contraction of part or all the affected LR belly in upward or downward target fixation by the fellow eye strongly suggests innervation of the LR by CN3 branches normally destined for the SR and IR, respectively, causing a horizontal strabismus that varied with vertical gaze position. Similar to CFEOM1,[11] the most common pattern was A or λ pattern strabismus, with relative exodeviation in downward gaze. Consistent with a prior electrophysiologic report,[29] MRI indicated that pattern strabismus in DRS is due to LR contraction in downward gaze, presumably because the LR is innervated by a branch of CN3 that normal innervates the IR.

The present study also confirms prior reports of absence of the subarachnoid CN6 in some cases of DRS. Kim and Hwang[9,30] have emphasized the frequent absence of CN6 ipsilateral to DRS type 1 and type 3,[9] but the presence of CN3 ipsilateral to type 2.[9] Three of four affected subjects imaged in the current study had bilateral absence of CN6, whereas CN6 was absent unilaterally in the fourth subject.

New Structural Findings in DURS2

The present study provides imaging evidence for LR innervation by a branch of CN3, including contractile thickening of the LR on attempted vertical gaze. Although MRI resolution is inadequate to confirm the presence of motor endplates in the LR, the inferior division of CN3 was consistently seen to run adjacent to the deep portion of the LR where CN6 normally enters and arborizes. We also found structural abnormality in the deep LR belly in DURS2. In DURS2, the deep LR was commonly split longitudinally into superior and inferior zones, or was even more structurally disorganized, similar to the structural abnormality in CFEOM1 resulting from mutations in *KIF21A*.[11] We propose that normal CN6 innervation is necessary for normal structure of the deep LR belly. Misrouting of

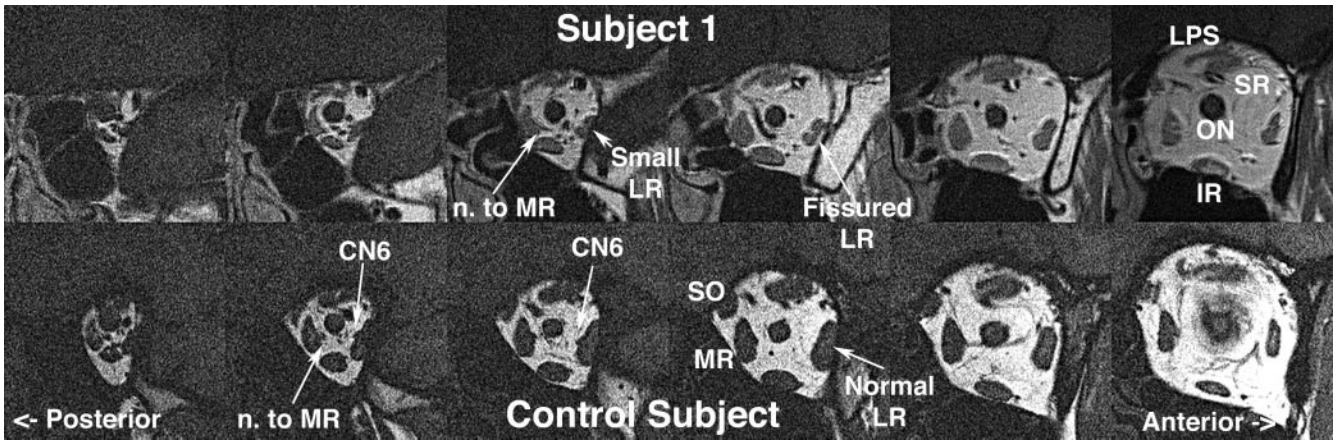

FIGURE 8. Coronal MRI of left orbit in planes 2-mm thick spaced by 2 mm, resolution 234 μm in plane. *Top row*: subject 1 with clinical phenotype of DRS unilateral type 3 on the right only. Note hypoplasia of the deep portion of the LR, without a recognizable abducens nerve (CN6). The LR is also fissured. Also evident is the motor nerve to the MR. *Bottom row*: normal control subject, showing a normal LR cross section.

CN3 in DURS2 is more likely the result of anatomic proximity than of inherent promiscuity of the nerve, and so it is the inferior zone of the LR that commonly receives aberrant innervation from CN3. It may be that CN3 is commonly misrouted to LR because CN3's normal path takes it adjacent to the LR's nerve entry site. No similar proximity of CN4 or CN6 occurs for other EOMs. However, other factors such as developmental timing may additionally or alternatively account for misinnervation of the LR.

In the present subjects with DURS2, the LR muscles demonstrated regional abnormalities, including hypoplasia and absent contractility in the deep portion of the EOM belly. Where present, CN6 entered the superior zone of the LR, whereas aberrant innervation from CN3 entered the inferior zone. This finding implies that the LR in DURS2 is a two-headed EOM, with each head separately innervated but joined to a common scleral insertion. This functional anatomic observation can explain the electromyographic observations of in DRS Scott and Wong,[29] who found evidence of two populations of LR motor units: the presumably normally innervated population activated during abduction, and an abnormally innervated population originally destined for the MR. These two populations presumably represent the two zones of the LR. More severe involvement of the deeper portions of EOMs is also seen in CFEOM1[11] and congenital oculomotor palsy,[31] suggesting that innervation may be a general organizing and trophic factor in the deep bellies of EOMs.

Although in the present study we examined IO volume in only three EOMs affected by DURS2, reduced IO volume in these cases suggests involvement. The maximum SO cross section in DURS2 was also significantly reduced. Although oblique EOM hypoplasia is a novel finding in DURS2, SO palsy has been reported to be associated in a family subgroup with DURS2.[27] Hypoplasia of the SO muscle is a hallmark of acquired and congenital SO palsy.[16,32] Oblique EOM palsy may represent neurogenic atrophy or hypoplasia.

Abnormalities were frequently found in the inferior division of CN3 as well as CN6 at its exit from the brain stem and in the orbit. Although hypoplasia and aplasia of CN6 were expected in at least some cases of DRS, hypoplasia of CN3 is novel. Hypoplasia of CN3 is characteristic of CFEOM1, which shares with DURS2 the findings of restricted vertical gaze and misrouting of CN3 branches to the LR to produce A- and V-pattern strabismus.[11] CFEOM1 is produced by missense mutations in the developmental kinesin *KIF21A*, whereas the cause of DURS2 is unknown. Endophenotypic similarity suggests that DURS2 and CFEOM1 share common pathogenetic mechanisms.

ON Involvement in DURS2

Quantitative MRI has emerged as a powerful technique for ON analysis.[24] subjects with CFEOM1 due to *KIF21A* mutations exhibit a subclinical 30% to 40% reduction in ON cross-sectional area.[11] ON cross-sectional area in the current subjects with DURS2 was reduced approximately 25% from normal. Our additional observation of ON hypoplasia suggests that the DURS2 gene also plays a role in the development or maintenance of the ON. Although the ON hypoplasia was statistically significant, it was not evident at ophthalmoscopy. None of the subjects with DURS2 had profound visual acuity loss, gross visual field deficits, or afferent pupillary defects. The current subjects with DRS exhibited little or no difference in best corrected visual acuity between eyes, indicating no or minimal amblyopia, and consistent with the reportedly low prevalence of amblyopia in DRS comparable to that in the normal population.[33]

Absence of Widespread Pulley Abnormalities

Pulley disorders are now recognized as causes of strabismus.[16,34] Abnormalities of rectus EOM paths due to misplaced pulleys are associated with craniosynostosis syndromes and are caused by mutations in *FGFR*[35] in which orbital nerves and EOM volumes are apparently normal. This contrasts with normal pulley positions in DURS2 and in CFEOM1.[11] Pulley positions can be normal despite abnormal innervation, supporting the idea that pulley abnormalities may be primary in cases of incomitant strabismus with which they are associated.[19,36,37]

Cocontraction of antagonist EOMs producing LR sideslip has been documented as a cause of up- and downshoots in DRS,[38] but was not observed here in DURS2. Several lines of evidence support misinnervation of rectus EOMs as the mechanism of anomalous ocular versions here. The LR in subject 1 exhibited evidence of segmental contraction in its anterior portion during attempted abduction, without appreciable contractile change in the deep orbit where normal contractility is maximal. In adduction, the right IR of subject 1 increased in cross section in a manner suggestive of contraction, but the normal coinfraductor, the SO, did not change cross section. Imaging in multiple gaze positions did not indicate rectus EOM sideslip.

Conclusions

Taken together, these findings indicate that DURS2 is a diffuse congenital cranial dysinnervation disorder affecting mainly CN6, but also producing misrouting of CN3 and ON hypoplasia. We speculate that structural abnormalities mainly of the LR belly in DURS2 are secondary to abnormal patterns of innervation.

References

1. Duane A. Congenital deficiency of abduction associated with impairment of adduction, retraction movements, contraction of the palpebral fissure and oblique movements of the eye. *Arch Ophthalmol*. 1905;34:133–159.
2. Huber A. Electrophysiology of the retraction syndromes. *Br J Ophthalmol*. 1974;58:293–300.
3. Strachan IM, Brown BH. Electromyography of extraocular muscles in Duane's syndrome. *Br J Ophthalmol*. 1972;56:594–599.
4. Miller NR, Kiel SM, Green WR, Clark AW. Unilateral Duane's retraction syndrome (type 1). *Arch Ophthalmol*. 1982;100:1468–1472.
5. Hotchkiss MG, Miller NR, Clark AW, Green WM. Bilateral Duane's retraction syndrome: a clinical-pathologic case report. *Arch Ophthalmol*. 1980;98:870–874.
6. Parsa CF, Grant E, Dillon WP, du Lac S, Hoyt WF. Absence of the abducens nerve in Duane syndrome verified by magnetic resonance imaging. *Am J Ophthalmol*. 1998;125:399–401.
7. Ozkurt H, Basak M, Oral Y, Ozkurt Y. Magnetic resonance imaging in Duane's retraction syndrome. *J Pediatr Ophthalmol Strabismus*. 2003;40:19–22.
8. Kim JH, Hwang J-M. Hypoplastic oculomotor nerve and absent abducens nerve in congenital fibrosis syndrome and synergistic divergence with magnetic resonance imaging. *Ophthalmology*. 2005;112:728–732.
9. Kim JH, Hwang JM. Presence of abducens nerve according to the type of Duane's retraction syndrome. *Ophthalmology*. 2005;112:109–113.
10. DeRespinis PA, Caputo AR, Wagner RS, Guo S. Duane's retraction syndrome. *Surv Ophthalmol*. 1993;38:257–288.
11. Demer JL, Clark RA, Engle EC. Magnetic resonance imaging evidence for widespread orbital dysinnervation in congenital fibrosis of extraocular muscles due to mutations in KIF21A. *Invest Ophthalmol Vis Sci*. 2005;46:530–539.
12. Demer JL, Ortube MC, Engle EC, Thacker N. High resolution magnetic resonance imaging demonstrates abnormalities of motor nerves and extraocular muscles in neuropathic strabismus. *J AAPOS*. 2006;10:135–142.
13. Evans JC, Frayling TM, Ellard S, Gutowski NJ. Confirmation of linkage of Duane's syndrome and refinement of the disease locus to an 8.8-cM interval on chromosome 2q31. *Hum Genet*. 2000;106:636–638.
14. Appukuttan B, Gillanders E, Juo SH, et al. Localization of a gene for Duane retraction syndrome to chromosome 2q31. *Am J Hum Genet*. 1999;65:1639–1646.
15. Engle EC, Andrews C, Law K, Demer JL. Two pedigrees segregating Duane's retraction syndrome as a dominant trait linked to the DURS2 genetic locus. *Invest Ophthalmol. Vis. Sci.* 2007;48:189–193.
16. Demer JL. A 12 year, prospective study of extraocular muscle imaging in complex strabismus. *J AAPOS*. 2003;6:337–347.
17. Demer JL, Miller JM. Orbital imaging in strabismus surgery. In: Rosenbaum AL, Santiago AP, eds. *Clinical Strabismus Management: Principles and Techniques.* Philadelphia: WB Saunders;1999:84–98.
18. Clark RA, Miller JM, Demer JL. Three-dimensional location of human rectus pulleys by path inflections in secondary gaze positions. *Invest Ophthalmol Vis Sci*. 2000;41:3787–3797.
19. Clark RA, Miller JM, Demer JL. Displacement of the medial rectus pulley in superior oblique palsy. *Invest Ophthalmol Vis Sci*. 1998;39:207–212.
20. Clark RA, Miller JM, Demer JL. Location and stability of rectus muscle pulleys inferred from muscle paths. *Invest Ophthalmol Vis Sci*. 1997;38:227–240.
21. Seitz J, Held P, Strotzer M, et al. MR imaging of cranial nerve lesions using six different high-resolution T1 and T2(*)-weighted 3D and 2D sequences. *Acta Radiologica*. 2002;43:349–353.
22. Kono R, Clark RA, Demer JL. Active pulleys: magnetic resonance imaging of rectus muscle paths in tertiary gazes. *Invest Ophthalmol Vis Sci*. 2002;43:2179–2188.
23. Demer JL, Oh SY, Clark RA, Poukens V. Evidence for a pulley of the inferior oblique muscle. *Invest Ophthalmol Vis Sci*. 2003;44:3856–3865.
24. Karim S, Clark RA, Poukens V, Demer JL. Quantitative magnetic resonance imaging and histology demonstrates systematic variation in human intraorbital optic nerve size. *Invest Ophthalmol Vis Sci*. 2004;45:1047–1051.
25. von Noorden GK. *Binocular Vision and Ocular Motility: Theory and Management of Strabismus.* St. Louis: Mosby; 1996.
26. Al-Baradie R, Yamada K, St Hilaire C, et al. Duane radial ray syndrome (Okihiro syndrome) maps to 20q13 and results from mutations in SALL4, a new member of the SAL family. *Am J Hum Genet*. 2002;71:1195–1199.
27. Chung M, Stout T, Borchert MS. Clinical diversity of hereditary Duane's retraction syndrome. *Ophthalmology*. 2000;107:500–503.
28. Sato S. Electromyographic study on retraction syndrome. *Jpn J Ophthalmol*. 1960;4:57–66.
29. Scott AB, Wong GY. Duane syndrome. *Arch Ophthalmol*. 1972; 87:140–147.
30. Kim JH, Hwang J-M. Usefulness of MR imaging in children without characteristic clinical findings of Duane's retraction syndrome. *Am J Neuroradiol.* 2005;26:702–705.
31. Wu J, Isenberg SJ, Demer JL. Magnetic resonance imaging demonstrates neuropathology in congenital inferior division oculomotor palsy. *J AAPOS.* 2006;10:473–475.
32. Demer JL, Miller JM. Magnetic resonance imaging of the functional anatomy of the superior oblique muscle. *Invest Ophthalmol Vis Sci*. 1995;36:906–913.
33. Tredici TD, von Noorden GK. Are anisometropia and amblyopia common in Duane's syndrome? *J Pediatr Ophthalmol Strabismus.* 1985;22:23–25.
34. Oh SY, Clark RA, Velez F, Rosenbaum AL, Demer JL. Incomitant strabismus associated with instability of rectus pulleys. *Invest Ophthalmol Vis Sci*. 2002;43:2169–2178.
35. Muller U, Steinberger D, Kunze S. Molecular genetics of craniosynostotic syndromes. *Graefes Arch Clin Exp Ophthalmol*. 1997;235:545–550.
36. Clark RA, Miller JM, Rosenbaum AL, Demer JL. Heterotopic muscle pulleys or oblique muscle dysfunction? *J AAPOS*. 1998;2:17–25.
37. Demer JL, Clark RA, Miller JM. Heterotopy of extraocular muscle pulleys causes incomitant strabismus. In: Lennerstrand G, ed. *Advances in Strabismology.* Burent, The Netherlands: Aeolus Press; 1999:91–94.
38. Miller JM, Demer JL, Rosenbaum AL. Two mechanisms of up-shoots and down-shoots in Duane's syndrome revealed by a new magnetic resonance imaging (MRI) technique. In: Campos EC, ed. *Strabismus and Ocular Motility Disorders.* London: Macmillian Press; 1990:229–234.